List of Publications:

1. Micellar Shape Transition under Dilute Salt-Free Conditions: Promotion and Self-Fluorescence Monitoring of Stimuli-Responsive Viscoelasticity by 1- and 2-Naphthols, Swapan K. Saha, Mrinmoy Jha, Moazzam Ali, Amitabha Chakraborty, Goutam Bit, and Susanta K. Das, ***J. Phys. Chem. B***, 2008,112,4642-4647.

2. Hydrogen-Bond-Induced Microstructural Transition of Ionic Micelles in the Presence of Neutral Naphthols: pH Dependent Morphology and Location of Surface Activity, Moazzam Ali, Mrinmoy Jha, Susanta K. Das, and Swapan K. Saha, ***J. Phys. Chem. B***, 2009,113,15563–15571.

3. Determination of unperturbed dimension and interaction parameters of sodium alginate in binary solvent mixtures by viscosity measurements, Mrinmoy Jha, Soumik Bardhan, Gulmi Chakraborty, Bidyut Debnath, Swapan K. Saha, ***J. Colloid Polymer Sc.,*** 2015 (Submitted)

4. Studies on Solution Properties of Poly (Vinyl Alcohol) in Water-Acetone and Water-Tetra Hydro Furan Mixtures, Mrinmoy Jha, Soumik Bardhan, Gulmi Chakraborty, Swapan K. Saha, ***J. Chem. Eng. Data,*** 2015 (Submitted)

Micellar Shape Transition under Dilute Salt-Free Conditions: Promotion and Self-Fluorescence Monitoring of Stimuli-Responsive Viscoelasticity by 1- and 2-Naphthols

Swapan K. Saha,* Mrinmoy Jha, Moazzam Ali, Amitabha Chakraborty, Goutam Bit, and Susanta K. Das

Department of Chemistry, University of North Bengal, Darjeeling 734 013, India

Received: October 9, 2007; In Final Form: February 2, 2008

Effect of 1 and 2-naphthols on the shape transition of cetyl trimethylammonium bromide (CTAB) and cetylpyridinium bromide (CPB) micelles are studied. Stimuli-responsive viscoelastic gels of long wormlike micelles are formed at low surfactant concentrations in the presence of neutral naphthols, where H-bonding plays a key role in micellar shape transition in the absence of any charge screening. Micelle-embedded naphthols also act as novel self-fluorescence probes for monitoring viscoelasticity of the system as a function of applied shear. ^{1}H NMR study shows that the solubilization sites of naphthols in the micelle are located near the surface. While UV absorption and Fourier transform infrared studies confirm the presence of intermolecular H-bonds in micelle embedded naphthols, transmission electron micrographs of vacuum-dried samples at room temperature demonstrate the transition in shape from sphere to rodlike micelles.

Introduction

Stimuli-responsive properties of viscoelastic gels of long wormlike micelles are fascinating and have created a great deal of interest in recent years.[1−4] Most extensively studied system is the cetyltrimethylammonium bromide (CTAB) micelles in presence of a hydrotrope, sodium salicylate (SS). Unlike simple halides, salicylate promotes sphere to wormlike micellar transition at very low concentrations, viz., near the normal critical micelle concentration (cmc, ~1 mM) of CTAB. The flexible and elongated wormlike micelles under dilute conditions show complex and unusual rheological phenomena, which include strong viscoelasticity and shear-induced structure (SIS) formation.[5−7] It is particularly interesting that, while a wide variety of wormlike ionic micellar solutions display identical rheological responses, a common element in most of these systems is the presence of salt anions such as SS. Although a few examples are available in the literature where additives other than SS have been used, these molecules have never been considered as high up as the promoter like SS.[8] However, a number of studies on micellar shape transition in cationic, anionic, and catanionic surfactant systems induced by polar and nonpolar organic species under comparatively high concentration conditions have been reported in the literature.[9−11] While hydrophobic molecules with either aromatic ring or small polar group have shown better efficiency, no unusual rheological feature was apparent under this condition. The presence of an anionic charge on the promoter molecule has been considered pivotal in achieving low concentration shape transition of cationic micelles via charge screening because it decreases the average area per surfactant head group allowing the packing parameter to exceed the critical value of $^1/_3$.[12] However, other important factors including the role of OH group of the promoter molecule have not attracted much attention, and as such, the puzzling question as to why not only its presence but also its position in the aromatic ring of SS molecule is so vital remains broadly unanswered.[13] Therefore, to understand the role of the OH group precisely, it was tempting to check what would happen if we use uncharged naphthols where the hydrophobic part is very strong and the anionic charge is absent. In this paper we have studied effect of neutral 1- and 2-naphthols on the shape transition of CTAB and CPB micelles and shown that intermolecular H bonding between OH groups of micelle embedded naphthol molecules plays a key role in micellar shape transition in absence of any charge screening of head groups and imparts strong viscoelasticity to the dilute aqueous surfactant solution.

* To whom correspondence should be addressed. E-mail: ssahanbu@hotmail.com.

Experimental

1-Naphthol(puriss) and 2-naphthol(puriss) (Aldrich products) were purified further by vacuum sublimation followed by recrystallization from 1:1 aqueous methanol. CTAB (puriss, Aldrich) and CPB (Aldrich) were used as received. ^{1}H NMR and Fourier transform infrared (FTIR) were recorded on a Bruker (300 MHz) spectrometer and a Shimadzu (083000) spectrometer, respectively. Steady-state fluorescence was measured on a Perkin-Elmer LS-55 luminescence spectrometer. UV absorption spectra were recorded on a Jasco (V-530) spectrophotometer. Shear-induced viscosity was measured on a rotational viscometer (Anton-Paar, DV-3P; accuracy ±1% and repeatability ±0.2%) equipped with temperature controller and with the facility of varying shear rates.

Results and Discussion

Shear-Induced Viscosity and Fluorescence Intensity. Aqueous CTAB or CPB (2−10 mM) and 1- or 2-naphthol (2−10 mM in 2−5% methanol, naphthols being sparingly soluble in water) solutions show viscosities similar to those of water. But as soon as these solutions are mixed together at room temperature, a thick gel-type fluid with high viscoelasticity is developed. Since viscoelasticity tends to disappear in high methanol concentrations, experimental solutions are prepared routinely by transferring the required amount of naphthol solutions (in pure methanol) in the experiment vial first, and

10.1021/jp709850u CCC: $40.75
Published on Web 03/22/2008

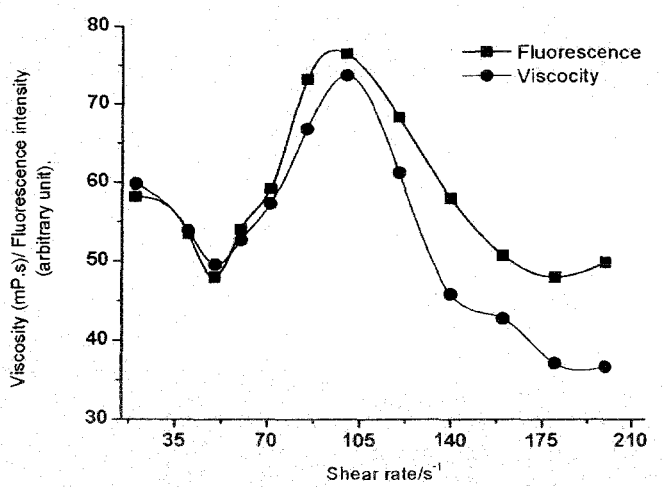

Figure 1. Variation of viscoelasticity of CPB−2-naphthol (10 mM) system with applied shear rate.

then the alcohol was evaporated off completely before the addition of aqueous surfactant solution. Much like the CTAB−SS system, CTAB−naphthols and CPB−naphthols also display maximum viscoelasticity at a 1:1 molar ratio of surfactant and the promoter. The argument that an excess or deficiency of charge on the micelles due to adsorption of hydrotrope anions (e.g., SS) would shorten the micellar life time and size is not apparently true for the present system because under the present experimental condition of solution pH (~6.5), the naphthols are mostly protonated, i.e., uncharged (pK_a's > 9.0). Therefore, it seems apparent that the symmetrical distribution of surfactant and the promoter molecules leading to highly compact spherical micelles facilitates an optimum surface curvature to attain in presence of H bonding (discussed later), and this results in the sphere to rod transition easily. For further experiments, naphthol to surfactant ratio was chosen to produce strongest viscoelasticity, i.e., 1:1 mole ratio. At low concentrations (<2 mM), CTAB or CPB−naphthol solutions show shear thinning properties, typically observed in the case of a non-Newtonian fluid. But at higher concentrations (>2 mM; 25 °C), present experimental systems display interesting rheological phenomenon. Up to the applied shear rate of ~52 s^{-1} (which is concentration dependent) for the CPB−2-naphthol system, solutions shear thin (Figure 1). An onset of viscosity rise is observed thereafter as a function of applied shear, and the viscosity share rate profile passes through a maximum, e.g., at 102 s^{-1} for the above system (Figure 1).

This behavior is consistent with building up of long wormlike micellar bundles.[7] The system recoils after the applied shear is withdrawn and takes a very long time (e.g., half-life period of viscosity decay of a CTAB−1-naphthol (7.0 mM) system equals ~56 min; samples were sheared in a rotational viscometer at 100s^{-1} for ≥5 min to ensure that the high viscosity regime was reached) to recoil completely and to return to an equilibrium unsheared state. Shear rates at which viscosity transition takes place and the shear rates at which maximum viscosity is displayed by various systems are shown in Table 1.

Systems which display shear induced nonlinear rheological changes (such as the present systems) bring about formidable problem in measuring unperturbed solution viscosity because the measuring techniques (e.g., torsional shear rheometry) often apply considerable stress on the system during measurement, and thus the zero-shear viscosity becomes obscure. Both the naphthols are well-known fluophores, and significantly, the quantum yield of emission of the naphthols is found to be very sensitive to the solution viscosity of the present systems. This

TABLE 1: Shear-Induced Viscoelastic Characteristics of CTAB and CPB Micelles in Presence of 1- and 2-Naphthols

viscoelastic system (10 mM, 1:1)	transition shear rate/s^{-1}	shear rate at maximum viscosity/s^{-1}
1-naphthol−CTAB	60	115
2-naphthol−CTAB	42	100
1-naphthol−CPB	63	106
2-naphthol−CPB	52	102

offers an interesting route for fluorescence monitoring of unperturbed viscosity as a function of applied shear. In a viscous medium, a fluophore cannot transfer energy efficiently via nonradiative means because of delayed collisions with the surrounding molecules resulting in the increased emission quantum yield. Moreover, the dipole moment of the probe in the excited state is greater than that in ground state, and hence interaction of the excited probe molecule with its surrounding molecules is different from that before absorption. Reorientation and translation of nearest-neighbor molecules allow the probe molecule to relax gradually to its equilibrium excited singlet state (S_1). In solutions of low viscoelasticity where these relaxations are very fast, fluorescence practically takes place from this equilibrium excited state S_1. In highly viscoelastic solutions, the relaxation of molecules surrounding the probe may be slow, and the probe molecules may emit before reaching their equilibrium excited state S_1, and a blue shift of the fluorescence spectrum may also be observed accompanying by an intensity enhancement. Similar situation is also encountered in a twisted intermolecular charge transfer state (TICT) formation where in a less viscous environment the probe molecules also display internal rotation and charge transfer, which results in the less emission quantum yield than that in a high viscous environment.[14,15] Furthermore, naphthols are weak acids in the ground state. In aqueous solution (pH ≈ 6.0−7.0), they exist almost completely in the acid forms. On excitation into the lowest singlet excited state, the pK_a values drop by several units (2-naphthol: $pK_a^* \approx 2.78$; 1-naphthol: $pK_a^* \approx 0.40$),[16−18] i.e., they undergo deprotonation in the excited state (DES).[19,20] As a result, the emission from the neutral forms of 1- and 2-naphthols at 360 and 357 nm, respectively, exhibits very low intensity than those of the anion forms near 450 or 420 nm, respectively. However, on binding to micelles, the DES process is restricted significantly causing a 20−90-fold increase in the intensity and life time of the neutral emission as well as in the rise time of the anion emission.[21] This is probably because of unavailability of an adequate number of water molecules in the vicinity of the naphthol molecules embedded inside the micelle to hydrate the proton released during photolytic deprotonation.[21] Therefore, at low surfactant concentrations (<2 mM; DES is significant), emissions from the deprotonated anion forms of the napthols were monitored at higher wavelengths, whereas in the presence of high concentrations of surfactant, emission from neutral form of 2-naphthol were monitored at lower wavelengths (where DES is insignificant) in the present experiments (1-naphthol shows very low quantum yield for neutral emission). Figure 1 also compares the shear induced viscosity data with that of fluorescence intensity of the present CPB−2-naphthol system. While the overall feature of the shear-induced viscosity profile is identical with that of the emission, they are not exactly superimposed on one another possibly because of the perturbation imposed on the system during viscosity measurement. However, we failed to observe any direct effect of applied shear on the DES process. This is apparent from the nonvariant ratio of emission intensities of protonated to deprotonated naphthols as a function of applied shear. This also indicates that the shear does not influence the availability of water molecules to hydrate

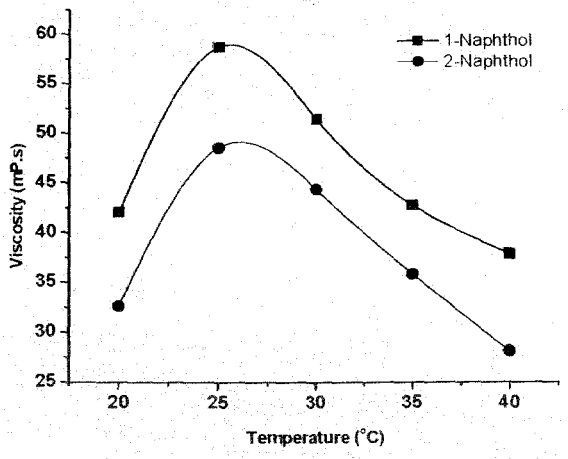

Figure 2. Variation of viscosity of CTAB−naphthol systems (10 mM; shear rate 30 s^{-1}) with temperature.

the liberated protons, i.e., the microstructure around the naphthol molecules in the wormlike micelles remains unchanged in SIS. However, as shown in Figure 1, it seems like that in the high applied shear rate (> 180 s^{-1}) the viscosity and fluorescence have opposite variation with the applied shear rate. Partial modification/disruption of wormlike micelles under high shear may change the compactness causing redistribution of naphthols in the micellar gel expelling some of the inner site naphthols to the outer site (better accessible to water molecules), resulting in the slight increase in the fluorescence intensity due to modified DES process.[22] In an experiment where hydrotropic promoter for micellar shape transition is not a fluophore, a probe must be added from the outside for the above measurement. This, in turn, may alter the hydrophobic trait of the system and affect the rheology. Therefore, one should be careful in using external fluorescence probes for monitoring viscosity.

Effect of Temperature. Typically, when a wormlike micellar solution is heated, the micellar contour length decays exponentially with temperature. At higher temperatures, surfactant unimers can move more rapidly between the cylindrical body and hemispherical end cap of the worm (the end cap is energetically unfavorable over the body by a factor equal to the end-cap energy). Thus, because end-cap constraint is less severe at higher temperatures, the worms grow to a lesser extent. However, an opposite trend in the rheological behavior is observed in CTAB/CPB−naphthol systems. Instead of a decrease in viscosity, it is increased with temperature steadily up to a critical temperature value (26 °C for CTAB−naphthols) and then decreases (Figure 2).

This transition as a function of temperature is reversible, i.e., if the temperature is lowered down from a high value, viscosity of the system follows the same viscosity−temperature profile. This observation is unusual, and the only example of this kind is found in a recent reference where wormlike micelle formation was promoted by sodium salt of hydroxy naphthalene carboxylate (SHNC).[23] However, any explanation emphasizing charge screening of surfactant head groups by the added salt anions as has been put forward in above experiments is not applicable. On the other hand, hydrophobic interaction between micellar core and the aromatic ring of the naphthol molecules seems to be an important factor, which imparts the thermoreversible viscoelastic property to the present system. As the temperature is increased, naphthol molecules (uncharged) are more soluble and perhaps are partitioned more strongly in the micellar phase. This favors the formation of longer wormlike micelles up to the critical temperature, above which the increased kinetic energy allowing surfactant unimers to hop more frequently

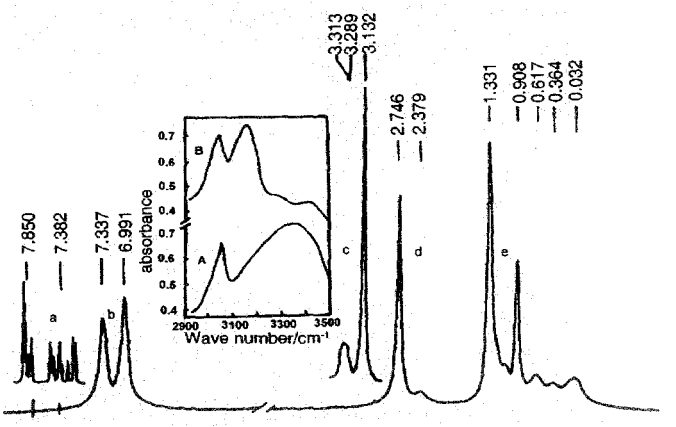

Figure 3. ^{1}H NMR and FTIR spectra of CTAB−2-naphthol system. (a) ^{1}H signal from 2-naphthol, (c) ^{1}H signal from CTAB, (b, d, e) NMR spectrum of CTAB−2-naphthol (1 mM, 1:1). Insets: FTIR spectra of 2-naphthol (A) in the absence of CTAB and (B) in the presence of CTAB.

between the body and the end cap results in the breaking up of the wormlike micelles.[23]

^{1}H NMR Study. To ascertain the location and orientation of the additive naphthol molecules in the micelles and to understand the nature of interaction in micellar shape transitions, ^{1}H NMR experiments were performed along with the absorption and emission spectroscopies. NMR spectrum of 2-naphthol in D_2O (in absence of CTAB) shows clusters of signals centered at δ values of 7.850 and 7.382, respectively, due to the resonance of the aromatic ring protons (Figure 3a). These two sets of signals are shifted upfield, broadened, and merged to give two broad signals at δ values of 7.337 and 6.991, respectively, when D_2O solution of CTAB and naphthols are mixed in 1:1 molar ratio (1.0 mM; Figure 3b). This large shift of aromatic proton resonance to low δ values clearly indicates the location of naphthol rings in the less polar environment than that of water. Previous studies with CTAB−SS system also showed similar upfield shift of proton resonance of the aromatic moiety of SS molecule, and it was argued that this was due to insertion of SS molecules into the micelles.[13] On the other hand, CH_3 protons of CTAB head group and the adjacent CH_2 protons, which resonate at 3.132 and 3.289, respectively, in D_2O (Figure 3c), are shifted upfield and resonate at 2.746 and 2.397, respectively, in the presence of 2-naphthol (Figure 3d). However, CH_2 protons adjacent to CTAB head group, are affected most in the presence of naphthols, and unlike pure CTAB, the signal from CH_2 protons emerges on the other side of CH_3 protons of CTAB head groups in the presence of naphthols. This identification is important because it indicates the presence of aromatic ring of naphthol near the surfactant head groups and close to adjacent CH_2 group. Signals from protons of other parts of hydrocarbon chain, however, remain unaffected in presence of naphthols (Figure 3e). The NMR spectra of 10 mM CTAB−2-naphthol (1:1) have further subtle features (Figure 4). While the signals from water protons remain well resolved (not shown), the signals from the aromatic protons of the naphthol molecules are broadened dramatically (Figure 4a). This means that on the NMR time scale, the motion of the naphthol molecules is highly restricted in viscoelastic phase, but water molecules rotate freely.[24] The signals from CTAB protons are, however, broadened to a lesser extent but appear structureless preventing further analysis (parts b and c of Figure 4). It seems that the naphthol molecules are held tightly in the micelles by means of strong hydrophobic interaction and H bonding. Above observation conclusively proves that the solubilized naphthol molecules are

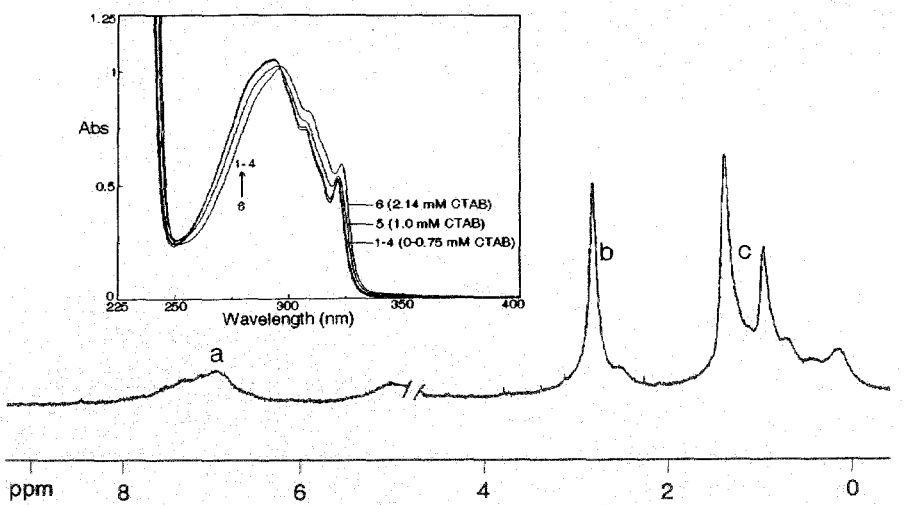

Figure 4. ^{1}H NMR and UV absorption spectra of CTAB−naphthol system: (a, b, c) NMR spectrum of CTAB−2-naphthol (10.0 mM, 1:1). Inset: UV absorption spectra of aqueous 1-naphthol (0.25 mM) solution at various CTAB concentrations.

penetrated not deep inside the micellar core but present near the surface probably with a well-defined orientation in which the OH groups are protruded from the micellar surface toward the polar aqueous phase. A previous study on the measurement of "apparent" shift of pK_a of 1-naphthol at the micellar surface of CTAB yielded an effective dielectric constant value of ~45, indicating that the location of OH groups of naphthol at the micellar surface is fairly polar in nature.[25,26]

UV Absorption and Emission Studies. Possibilities of the H bonding and $\pi-\pi$ interaction in naphthols have been checked by observing the effect of CTAB micelles on the absorption spectrum. The near-UV absorption of 1-naphthol (250−335 nm), which arises from two strongly overlapping $\pi-\pi^*$ transition, viz., $^1L_a \leftarrow {}^1A_1$ and $^1L_b \leftarrow {}^1A_1$, however, remains unaffected in presence of submicellar aqueous CTAB solution (Figure 4, inset) indicating absence of any appreciable interactions. But interestingly, a significant red-shift is observed in the spectrum at 293, 307, and 321 nm in presence of CTAB just above its cmc (1.0 mM) with a well-defined isobestic point at 296 nm. Previously, a similar red-shift of absorption spectrum of 2-naphthol in AOT reverse micelle relative to the spectrum of free naphthol was observed when this molecule acts as hydrogen-bond donor because of the perturbation by the negative charge carried on oxygen atom of the partner molecule.[27] The same reasoning applies to the present case also and the nature of spectral change indicates in favor of H bonding between naphthol molecules (red-shift is observed in 2-naphthol−CTAB system also), which are embedded increasingly in the micelle as the CTAB concentration (> 1.0 mM) is increased (Figure 4, inset).

It has been reported that fluorescence quenching can be induced by the hydrogen-bonding interactions for fluophores in the hydrogen-bonding surroundings and is explained by the hydrogen-bonding dynamics in the fluorescence state.[28−33] Therefore, it may be presumed that intermolecular H bonding in micelle-embedded naphthols can be studied effectively by observing fluorescence quenching (static and dynamic). However, excited-state proton transfer (ESPT) or DES process of hydroxy aromatic compounds such as naphthols seems to make the situation somewhat difficult. The ESPT rates of these compounds in aqueous solutions are limited by the time water takes to wrap itself around the charge because a water cluster of 4 ± 1 molecules is the proton acceptor in each case.[34] The first two steps in the ESPT process are, therefore, (i) the H-bonded complex formation of electronically excited state of naphthols with water molecules and (ii) hydrogen-bonded

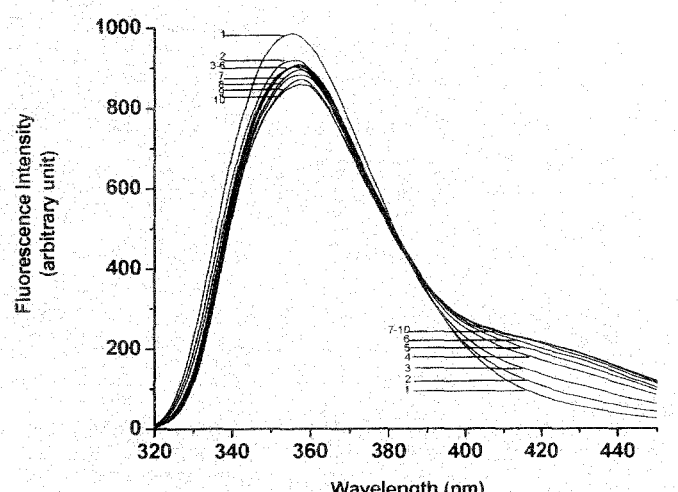

Figure 5. Fluorescence spectra of 2-naphthol (0.25×10^{-5} mol/L) in aqueous CTAB solutions in presence of 0.1 M HCl. [CTAB]: (1) 0.0 mM, (2) 3 mM, (3) 2.5 mM, (4) 2 mM, (5) 1.5 mM, (6) 1 mM, (7) 0.75 mM, (8) 0.5 mM, (9) 0.25 mM, and (10) 0.12 mM.

complex formation with water clusters required for protolytic dissociation.[19] ESPT process of 1- and 2-naphthols in organized media including different micelles have been investigated in considerable detail, but the results are not always unambiguous.[19,20,35,36] It has been shown that the ultrafast proton-transfer processes in ESPT became significantly retarded for 1-naphthol in micelles due to lack of water availability (as has already been mentioned), and the decay of the emissions are often multiexponential due to different solubilization sites in anionic and nonionic micelles, although a monoexponential decay process has also been observed for similar systems.[35,36] On the other hand, for CTAB micelles, the retardation effect is somewhat compensated by the catalytic effect of the micellar potential.[36] Although a previous study did not find convincing evidence that all of the naphthols in micelle are definitely in the form of H-bonded complex with several water molecules, which is required for photodissociation, possible existence of intermolecular H bond in electronically excited states of naphthols under identical condition of wormlike micelle formation have been re-examined in the present study.[19] Figures 5 and 6 show the emission spectra of 2- and 1-naphthols, respectively, in 0.1 M HCl in presence of CTAB. Addition of high excess of hydroxonium ion is to shift the acid−base equilibrium toward neutral naphthol (protonated) to facilitate intermolecular H-bond

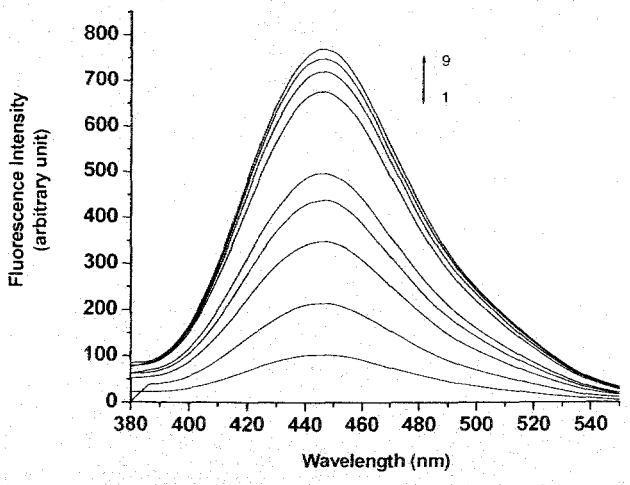

Figure 6. Fluorescence spectra of 1-naphthol (0.25×10^{-5} mol/L) in aqueous CTAB solutions in presence of 0.1 M HCl. [CTAB]: (1) 0.0 mM, (2) 0.25 mM, (3) 0.5 mM, (4) 0.75 mM, (5) 1.0 mM, (6) 1.5 mM, (7) 2.0 mM, (8), 2.5 mM, and (9) 3.0 mM.

formation. While 1-naphthol exhibits only anion emission ($pK_a^* \approx 0.40$), which is enhanced substantially in presence of CTAB, emission from 2-naphthol in water was essentially from the neutral naphthol molecules under the above condition ($pK_a^* \sim 2.78$). The effect of CTAB concentration on neutral as well as the anion emission of 2-naphthol is interesting (Figure 5). While addition of CTAB in the submicellar concentration range increases the intensity at ~420 nm region depicting catalytic effect of CTAB charge on the excited-state deprotonation, further addition of CTAB above the cmc (>1 mM) decreases the emission intensity indicating a retardation of the deprotonation rate for the lack of water availability in the micelles. Intensity of neutral emission, however, is increased slightly on the addition of CTAB in the submicellar concentration range, while in the post-micellar concentration range no appreciable change of emission intensity is observed. Moreover, no detectable shift of neutral emission wavelength or the fluorescence quenching on CTAB addition is observed. Therefore, neither any extensive disruption of H bonds that might exist between the electronically excited state of naphthols and the water clusters nor the formation of new intermolecular H bond among the embedded naphthols in the photoexcited state is obvious from the above result.

FTIR and Transmitting Electron Microscopic (TEM) Studies. The FTIR spectra of 2-naphthol in the presence and absence of CTAB micelles are shown in Figure 3 (insets A and B). The spectra of vacuum-dried samples (25 °C) provided interesting results (in KBr pellets). (Studying the spectral feature of OH group of naphthols in aqueous solution was not possible (in CaF_2 cell) due to overlapping of IR peaks with that of water.) The broad band around 3354 cm^{-1}, which is assigned to the OH stretching of 2-naphthol (typically observed in phenols) is shifted to 3163 cm^{-1} due to partitioning in the micelles. Comparatively sharper peak at higher wavelength confirms the presence of well-defined and stronger H bond in naphthols, which are embedded inside CTAB micelles. The peak at 3050 cm^{-1}, which remains almost unchanged upon gelation, may be assigned to aromatic CH stretch. Above shifting of OH stretching frequency is very much reproducible and consistently displayed by a wide variety of wormlike micellar systems promoted by naphthols. It seems apparent that H bonding plays an important role in micellar shape transition.[37] The result also shows that vacuum drying at room temperature did not destroy the microstructure completely although may have modified it

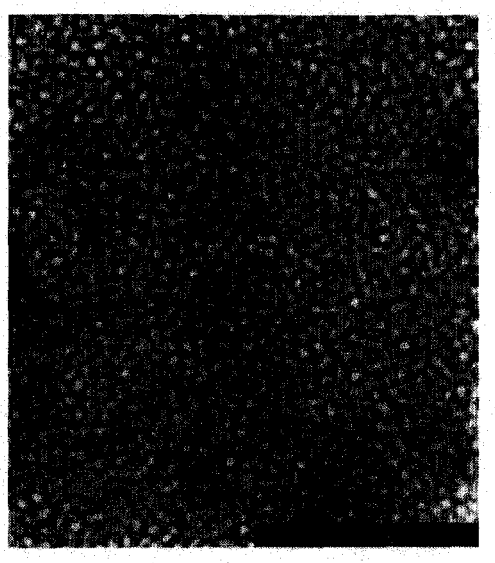

Figure 7. TEM micrographs of CTAB−2-naphthol system (10 mM, 1:1).

to some extent. This observation is also supported by TEM experiments done under identical conditions. The sample preparation on TEM grid was done according to the method described elsewhere followed by vacuum drying at room temperature as above.[38] The TEM micrograph looks like a condense, isotropic, and continuous network (Figure 7). The structure represents the transition in shape from spherical to rodlike micelles. Interestingly, this TEM picture is almost identical with that of the microstructure observed under cryoTEM for cetyltrimethylammonium hydroxide (100 mM) in presence of 2-hydroxy 1-naphthoic acid (55 mM) by a previous worker.[39] Freeze-fracture electron microscopy done with CTAB-SS system also indicated the formation of isotropic wormlike micelles similar to one shown in Figure 7,[5] along with other morphologies. This result clearly suggests that specific and stronger H bonds are formed between naphthol molecules, which are embedded in micelles because of their close proximity. In absence of charge screening, these H bonds force to decrease the surface area per surfactant head group causing micellar shape transition to occur. In the presence of hydrotropes like SS, however, both the phenomena, viz., charge screening as well as H bonding may be operative simultaneously.

Conclusion

Stimuli-responsive viscoelastic gels of long wormlike CTAB and CPB micelles are formed at low surfactant concentrations in presence of 1- and 2-naphthols. In the absence of charge screening of surfactant head groups, H bonding among micelle-embedded naphthol molecules probably plays the key role in micellar shape transition. Micelle-embedded naphthols act as novel self-fluorescence probes for monitoring viscoelasticity as a function of applied shear. The viscoelastic gels formed in presence of naphthols are thermoreversible in nature, and the viscosity−temperature profile of each system passes through a maximum. ^1H NMR confirms that solubilization sites of naphthols in the micelle are located near the surface. The above study also shows that, on the NMR time scale, the motion of the naphthol molecules is highly restricted in viscoelastic phase, but water molecules rotate freely. While fluorescence quenching via H-bond strengthening is not observed in the micellar phase, UV absorption spectra demonstrate the presence of inter-

molecular H bond in micelle-embedded naphthols in their ground electronic states, which was confirmed by FTIR. The ESPT of 2-naphthol is facilitated in presence of CTAB in the submicellar concentration range due to the catalytic effect of surfactant charge where as, ESPT is hindered in postmicellar concentrations due to lack of water accessibility. TEM micrographs of vacuum-dried samples demonstrate spherical to rodlike micellar transition of CTAB and CPB in presence of naphthols, as seen in Figure 7.

Acknowledgment. This work was funded by the Council of Scientific and Industrial Research, New Delhi.

References and Notes

(1) Rehage, H.; Hoffmann, H. *J. Phys. Chem.* **1988**, *92*, 4712−4719.
(2) Rehage, H.; Hoffmann, H. *Mol. Phys.* **1991**, *74*, 933−943.
(3) Cates, M.; Candau, S. J. *J. Phys.: Condens. Matter* **1990**, *2*, 6869−6877.
(4) Hu, Y.; Rajaram, C. V.; Wang, S. Q.; Jamieson, A. M. *Langmuir* **1994**, *10*, 80−85.
(5) Keller, S. L.; Boltenhagen, P.; Pine, D. J.; Zasadzinski, J. A. *Phys. Rev. Lett.* **1998**, *80*, 2725−2728.
(6) Boltenhagen, B.; Hu, Y.; Matthys, E. F.; Pine, D. J. *Phys. Rev. Lett.* **1997**, *79*, 2359−2362.
(7) Liu, C.; Pine, D. J. *Phys. Rev. Lett.* **1996**, *77*, 2121−2124.
(8) Manohar, C. In *Micelles, Microemulsions, and Monolayers; Science and Technology*; Shah, D. O., Ed.; Marcel Dekker, Inc.: New York, 1998; p 145.
(9) Lindemuth, P. M.; Bertrand, G. L. *J. Phys. Chem.* **1993**, *97*, 7769−7773.
(10) Hedin, N.; Sitnikov, R.; Furo, I.; Henriksson, U.; Regev, O. *J. Phys. Chem. B* **1999**, *103*, 9631−9639.
(11) Yin, H.; Lei, S.; Zhu, S.; Huang, J.; Ye, J. *Chem.−Eur. J.* **2006**, *12*, 2825−2835.
(12) Israelachivli, J. N.; Mitchell D. J.; Ninham, B. W. *J. Chem. Soc., Faraday Trans.* **1976**, *72*, 1525−1568.
(13) Rao, U. R. K.; Manohar, C.; Valaulikar, B. S.; Iyer, R. M. *J. Phys. Chem.* **1987**, *91*, 3286−3291.
(14) Kung, C. E.; Reed, J. K. *Biochemistry* **1986**, *25*, 6114−6121.
(15) Retting, W.; Lapouyade, R. In *Topics in Fluorescence Spectroscopy*; Lakowicz, J. R., Eds.; Plenum Press: New York, 1994; Vol. 4, p 109.
(16) Webb, S. P.; Yeh, S. W.; Philips, L. A.; Tolbert, M. A.; Clark, J. H. *J. Am. Chem. Soc.* **1984**, *106*, 7286−7288.
(17) Harris, C. M.; Selinger, B. K. *J. Phys. Chem.* **1980**, *84*, 1366−1371.
(18) Harris, C. M.; Selinger, B. K. *J. Phys. Chem.* **1980**, *84*, 891−898.
(19) Solntsev, K. M.; Ilichev, Y. V.; Demyashkevich, A. B.; Kuzmin, M. G. *J. Photochem. Photobiol. A* **1994**, *78*, 39−48.
(20) Ilichev, Y. V.; Demyashkevich, A. B.; Kuzmin, M. G. *J. Phys. Chem.* **1991**, *95*, 3438−3444.
(21) Sukul, D.; Pal, S. K.; Mandal, D.; Sen, S.; Bhattacharya, K. *J. Phys. Chem. B* **2000**, *104*, 6128−6132.
(22) Pappayee, N.; Mishra, A. K. *Photochem. Photobiol.* **2001**, *73*, 573−578.
(23) Kalur, G. C.; Frounfelker, B. D.; Cipriano, B. H.; Norman, A. I.; Raghvan, S. R. *Langmuir* **2005**, *21*, 10998−11004.
(24) Tata, M.; John, V. T.; Waguespack, Y. Y.; McPherson, G. L. *J. Phys. Chem.* **1994**, *98*, 3809−3817.
(25) Grieser, F.; Drummond, C. J. *J. Phys. Chem.* **1988**, *92*, 5580−5593.
(26) Das, S. K. Ph.D. thesis, University of North Bengal, India, 2006.
(27) Bardez, E.; Monnnier, E.; Valeur, B. *J. Colloid Interface Sci.* **1986**, *112*, 200−207.
(28) Das, S.; George Thomas, K.; Ramanathan, R.; George, M. V. *J. Phys. Chem.* **1993**, *97*, 13625−13628.
(29) Zhao, G.; Han, K. *J. Phys. Chem. A* **2007**, *111*, 2469−2474.
(30) Zhao, G.; Han, K. *J. Phys. Chem. A* **2007**, *111*, 9218−9223.
(31) Zhao, G.; Liu, J.; Zhao, L.; Han, K. *J. Phys. Chem. B* **2007**, *111*, 8940−8945.
(32) Samant, V.; Singh, A. K.; Ramakrishna, G.; Ghosh, H. N.; Ghanty, T. K.; Palit, D. K. *J. Phys. Chem. A* **2005**, *109*, 8693−8704.
(33) Zhao, G. *J. Chem. Phys.* **2007**, *127*, 024306−024306.
(34) Lee, J; Robinson, G. W.; Webb, S. P.; Philips, L. A.; Clark, J. H. *J. Am. Chem. Soc.* **1986**, *108*, 6538−6542.
(35) Mandal, D.; Pal, S. K.; Bhattacharyya, K. *J. Phys. Chem. A* **1998**, *102*, 9710−9714.
(36) Abou-al Einin, S.; Zaitsev, A. K.; Zaitsev, N. K.; Kuzmin, M. G. *J. Photochem. Photobiol. A* **1988**, *41*, 365−373.
(37) Waguespack, Y. Y.; Banerjee, S.; Ramannair, P.; Irvin, G. C.; John, V. T.; McPherson, G. L. *Langmuir* **2000**, *16*, 3036−3041.
(38) Liu, Z.; Cai, J. J.; Scriven, L. E.; Davis, H. T. *J. Phys. Chem.* **1994**, *98*, 5984−5993.
(39) Abdel-Rahem, R. Ph.D. thesis, University of Bayreuth, Germany, 2003.

Hydrogen-Bond-Induced Microstructural Transition of Ionic Micelles in the Presence of Neutral Naphthols: pH Dependent Morphology and Location of Surface Activity

Moazzam Ali, Mrinmoy Jha, Susanta K. Das, and Swapan K. Saha*

Department of Chemistry, University of North Bengal, Darjeeling 734 013, India

Received: August 9, 2009

The effect of naphthols and methoxynaphthalenes on the microstructure transition of cetyltrimethylammonium bromide (CTAB) micelles is studied. Although the surface activities of these two types of organic dopants are strong, methoxynaphthalenes failed to promote spherical to worm-like micellar transition and to impart viscoelasticity to the aqueous CTAB solution, presumably due to their inability to form unique H-bonds with interfacial water. The micropolarity of OH sites of micelle-embedded naphthols is measured by observing the pK_a shift at the micellar surface relative to bulk water. On the basis of spectroscopic and other data, the microstructures formed by both classes of dopants at the micellar surface are predicted. On the basis of hydroxyaromatic dopants, a simple and effective route to design pH-responsive viscoelastic worm-like micelles and the vesicles of single tail cationic surfactant (CTAB) is reported. Results are confirmed by observing cryogenic transmission electron microscopy (cryo-TEM) images.

Introduction

Organic π-conjugated molecules are effective tuners in the formation of various nanostructured materials, and the entailed route is potentially facile and efficient for the development of functional materials of technological and biological importance.[1−4] Microstructural transitions of micellar aggregates, especially the nature of transition from ordinary micelles to long worm-like giant micelles and the vesicles, mediated by organic π-electron systems are of fundamental scientific interest and have been reported in several papers recently.[5−8] Moreover, synthetic vesicular systems are interesting from a number of standpoints, not the least being their structural similarity with the constituent of the biomembrane, viz., phospholipid. They offer a convenient way to probe interactions involving membrane systems. Vesicle aggregation or adhesion is the primary step for the fusion of the vesicles in membrane. Therefore, the elucidation of the molecular mechanism of vesicular aggregation would greatly contribute to a better understanding of these biological phenomena. Single chain ionic surfactants, e.g., cetyltrimethylammonium bromide (CTAB), favor convex-up surface geometry of the micelles due to strong headgroup repulsion and form spherical or near spherical micelles at the critical micelle concentration (cmc), while either at much higher surfactant concentrations (~1.0 M) or in the presence of high inorganic salt concentrations (>0.1 M), morphological changes occur to rod-like micelles and vesicles.[9−12] Hydrotropic salts like sodium salicylate (SS) also promote sphere to worm-like micellar transition at considerably lower concentration (e.g., ~1.0 mM in CTAB) by increasing the packing parameter above the critical value of 1/3 via efficient charge screening of the surfactant head groups.[13] These worm-like micellar solutions at low concentrations show complex and unusual rheological phenomena. They exhibit some fascinating shear dependent properties and have been the subject of much discussion for a long time.[14−18] For example, when sheared below a critical shear rate which depends on temperature, surfactant, and salt concentrations, dilute worm-like micellar solutions shear thin. On the contrary, above a critical shear rate, micellar solutions show time dependent behavior. Initially, the solutions shear thin, and after an induction period, the solutions exhibit a shear thickening property. It has been suggested that shear thickening occurs because free worm-like micelles join a transient network under shear; the microstructures have been broadly named shear-induced structure or phase (SIS or SIP, respectively).[19−21] However, in certain systems, e.g., cetyltrimethylammonium chloride/sodium 3-methyl salicylate dispersion, vesicle to worm-like micellar transition and vice versa have been claimed to occur under shear, leading to rheological modification of the system.[22] A recent discovery of the flow-induced structure transition between vesicle and micelle is also interesting. The structural transition induced by flow in the cetyltrimethylammonium 3-hydroxy naphthalene 2-carboxylate micelles and the mixture of hexadecylpydinium chloride and sodium chlorate caused initial confusion because there has been apparently no reason for how the structural transition takes place.[22,23] As has already been pointed out, a facile and interesting route of lowering the surface curvature of micelles of single chain cationic surfactants is to increase the effective cross-sectional area of the hydrocarbon tail and to shield the headgroup charges by embedding neutral aromatic compounds with hydrogen bonding functionalities (e.g., 1- and 2-naphthols).[5] These dopants upon embedding in the micelle hinder any curvilinear displacement of head groups to take place via a comparatively rigid network of hydrogen bonding at the micelle surface and at the same time decrease the area of the surfactant head groups efficiently. The efficiency of hydroxy aromatic compounds in micellar shape transition is very high, and an aqueous mixture of CTAB and 2,3-dihydroxy naphthalene which gives highly viscous rod-like nanoaggregates has been used as a template for the sol−gel synthesis, providing an aqueous route for tube silicate preparation.[7] Altering the structure of the micellar system by phenolic dopant is an easy way to tailor the structure and properties of mesoporous materials which are synthesized on the micellar templates.[24] UV absorption spectra are modified due to the presence of an intermolecular H-bond in micelle-embedded naphthols in their ground elec-

* To whom correspondence should be addressed. E-mail: ssahanbu@hotmail.com.

10.1021/jp907677x CCC: $40.75
Published on Web 10/28/2009

tronic states, and this was confirmed by FTIR. The excited state proton transfer (ESPT) of 2-naphthol is facilitated in the presence of CTAB in the submicellar concentration range due to the catalytic effect of surfactant charge, whereas ESPT is hindered in post-micellar concentrations due to lack of water accessibility. However, the exact nature of H-bonding in the micellar phase is not understood completely. Moreover, together with hydrogen bonding, the $\pi-\pi$ and cation$-\pi$ interactions between favorably arranged micelle-embedded naphthol molecules may also be involved in modifying the absorption spectra.[25] Therefore, in order to further examine the exact nature of the noncovalent interaction that is involved in the above modification of the spectra, it is tempting to check what would happen if we replace the hydroxyl group of the promoter naphthol molecules by methoxy groups. Methoxy naphthalenes (MN) possess a similar structure and hydrophobicity to that of the naphthol (HN) molecules but cannot act as hydrogen bond donors. It would be interesting to compare the efficiency of methoxy naphthalenes with that of naphthols in effecting microstructural transitions of micelles and to discuss the result in the light spectroscopic observations. Further, it may be anticipated that a simple and effective route to design a pH-responsive microstructure could well be based on the neutral naphthol dopants, which form salts only at high pH ($pK_a > 9.2$). As a function of pH, ionization of the OH group of naphthol molecules may switch the onset of charge screening, paving the way to effect further morphological transitions (viz., vesicle formation). An objective of the present work is, therefore, to design a simple effective route of pH-responsive morphological transition for the aqueous molecular aggregates of single chain cationic surfactant, viz., CTAB from micelles to long worm-like micelle to unilamelar vesicles.

Finally, it is important to note that although the last two decades have witnessed a strong excitement among the researchers on the microstructural transitions of micelles at low concentrations, induced by hydrotropes like sodium salicylate and other similar dopants, leading to stimuli-responsive viscoelasticity, the exact role and the location of the protruded polar groups (e.g., OH groups) of the hydrotropes toward the Stern layer have not been firmly ascertained. This is particularly an interesting basic element to investigate for the present system where intermolecular H-bonding through OH groups of the micelle-embedded naphthols seems to play the pivotal role in the transition of the micellar morphology. In this work, therefore, micropolarity has been determined at the OH group sites by monitoring the pK_a shift at the micellar interface relative to bulk water in an attempt to determine the location of the protruded OH groups in the Stern layer.[26,27]

Experimental Section

1- and 2-Naphthols (puriss, Aldrich) were purified by vacuum sublimation followed by crystallization from 1:1 aqueous methanol. 1- and 2-Methoxynaphthalenes (Acros-Organics, Belgium) were recrystallized from 1:1 aqueous methanol before use. CTAB (puriss, Aldrich) was used as received. ^{1}H NMR and UV absorption spectra were recorded on a Bruker (300 MHz) spectrometer and a Jasco (v-530) spectrophotometer, respectively. Shear-induced viscosity was measured on a rotational viscometer (Anton-Paar, DV-3P; accuracy ±1% and repeatability ±0.2%) equipped with a temperature controller and with the facility of varying shear rates. A Kruss tensiometer (K 9) was used for surface tension measurements. Sample preparation on a TEM grid for cryo-TEM study was done following a similar method to that described in a previous paper.[5]

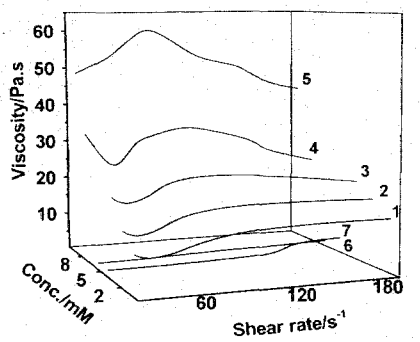

Figure 1. Steady shear viscosity as a function of the applied shear rate for dilute and concentrated solutions of 2-naphthol/CTAB at 25 °C. The molar concentration ratio, [2-naphthol]/[CTAB], was fixed at unity. (1) 1.0, (2) 1.5, (3) 2.0, (4) 5.0, (5) 8.5 mM. (6) and (7) are plots for 1- and 2-methoxynaphthalene−CTAB (5 mM, 1:1) systems, respectively.

Results and Discussion

Shear-Induced Viscoelasticity and Surface Activity: Role of the OH Group of the Dopant. Figure 1 shows the rheological responses for a representative viscoelastic system, viz., an aqueous CTAB−1-naphthol system as a function of concentration (1:1 mol ratio; this composition yields the strongest viscoelasticity) at 25 °C (pH ~5.0). At low concentrations (<2 mM), this system shows a shear thinning property up to a shear rate of 25 s^{-1} and then the shear thickening phenomenon starts to occur, but above a shear rate of 60 s^{-1}, the fluid shows a Newtonian type behavior (Figure 1(1,2)). However, an overall non-Newtonian nature is apparent as the concentration of the CTAB and naphthol (1:1) system is raised above 2.0 mM. At still higher concentrations (>5.0 mM), the nature of the rheological response changes dramatically and the system starts displaying an unusual rheology as a function of shear rate (Figure 1(4)). Up to a shear rate of 60 s^{-1}, the fluid shear thins. An onset of viscosity rise is observed at the shear rate of 60 s^{-1}, and the system again shear thins, passing through a maximum at 70 s^{-1}. At further higher concentrations (8.5 mM), the viscosity−shear rate profile again changes feature; the initial shear thinning characteristics disappear. The overall behavior is consistent with building up of long worm-like micellar bundles at relatively high concentrations. Therefore, it appears that the shear thinning viscosity in low shear rates is indicative of the flow-induced alignment toward the flow directions. Meanwhile, when the CTAB concentration is above 10.0 mM in the equimolar CTAB/naphthol solutions, the micelles are much longer and entangled with each other in the solution. In this case, the shear viscosity increases much higher and the micellar solution behaves like entangled polymer solutions exhibiting typical nonlinear viscoelastic behavior such as a stress plateau. The contour length of the worm-like micelles is highly dependent on the concentrations of the surfactant and the promoter.

The methoxynaphthalene−CTAB systems, on the other hand, neither display the ability to develop viscoelasticity (6,7 of Figure 1) in the system nor exhibit any viscosity modification with applied shear, and behave completely like a Newtonian liquid. This result is quite surprising in view of the fact that much like 1- and 2-naphthols, both 1- and 2-methoxynaphthalene are expected to embed into the micelles of CTAB. Therefore, to ascertain the location and orientation of the additive methoxy naphthalene molecules in the micelles and to understand the nature of the interaction with micelles, ^{1}H NMR experiments were performed (Figure 2).

The NMR spectrum of 1-MN in D_2O (in the absence of CTAB) shows four sets of signals, centered at δ values of 8.151,

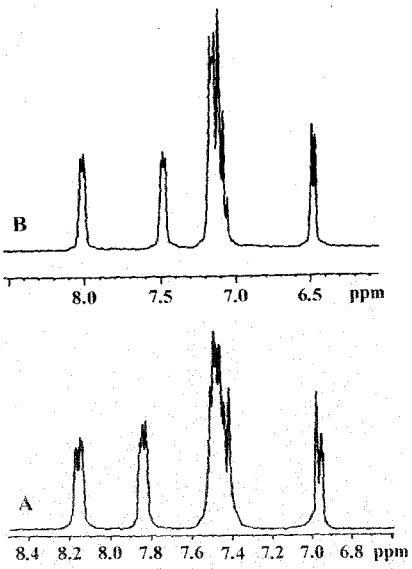

Figure 2. ^{1}H NMR spectra of 1-methoxynaphthalene in the absence (A) and presence (B) of CTAB (7.5 mM, 1:1).

7.853, 7.482, and 6.947, respectively, due to the resonance of the aromatic ring protons (Figure 2A). All four sets of signals are shifted upfield, remain well resolved, and appear at δ values of 8.013, 7.492, 7.147, and 6.487, respectively, when D_2O solutions of CTAB and 1-MN are mixed in 1:1 molar ratio (7.5 mM; Figure 2B). The methoxy protons which resonate at a δ value of 3.953 in water (not shown) are also shifted upfield and resonate at a δ value of 3.561 in CTAB. A similar upfield shift of aromatic and methoxy proton signals is observed in the CTAB−2-MN system as well. This large shift of either aromatic proton resonance or methoxy proton resonance to low δ values clearly indicates the location of naphthalene rings as well as the methoxy group of methoxy naphthalene molecules in the less polar environment than that of water. A previous study with the CTAB−naphthol system also showed a similar upfield shift of proton resonance of the aromatic moiety of the naphthol molecule, and it was argued that this was due to insertion of naphthol molecules into the micelle.[5] Unlike naphthol−CTAB systems, absence of line broadening and the well resolved structures of the NMR signals clearly indicates fast rotation of naphthalene rings in the CTAB−MN systems (on the NMR time scale). However, the degree of upfeild shift of the signals is less in 1-MN than that in naphthols; this indicates a stronger partitioning of naphthol molecules in the micelles. In this context, comparison of surface activities of methoxynaphthalenes and naphthols may also be interesting.

Figure 3 clearly shows that both 1- and 2-naphthols reduce the surface tension (ST) of water to a considerable extent, indicating that naphthols are surface active. Previously, it has been shown that 3-hydroxynaphthalene 2-carboxylate (SHNC) also reduces the surface tension in a similar manner and it also effectively promotes micellar shape transition.[28] Interestingly, while SHNC decreased the surface tension of water from a value of 75 to 60 N/m in the presence of 60 mM concentration of SHNC, an identical decrease in surface tension has been brought about by naphthols in the presence of only 0.4 and 0.5 mM concentrations. On the other hand, the surface tension of water is decreased to a similar extent by an even lesser amount of 1- and 2-MN's. While 1-MN decreases the ST of water up to the extent of 58 mN in the presence of 0.31 mM concentration, 2-MN did the identical ST lowering in the presence of only 0.16 mM concentration. While the extents of surface activity displayed by both naphthols are very close to each other, for 1- and 2-MN molecules, it differs quite significantly (Figure 3). The result indicates that 1- and 2-methoxy naphthalenes are stronger surface active agents than 1- and 2-naphthols, and accordingly, these molecules are expected to be embedded into the micelle strongly. Therefore, the findings of the NMR experiment are further strengthened by this fresh evidence of surface activities exhibited by methoxy naphthalene molecules. However, in spite of the strong surface activity shown by 1- and 2-MN, they fail to induce a microstructural transition in CTAB micelles. It seems apparent that OH groups in naphthol molecules play an important role in this respect. The results show that the naphthols are involved in a stronger and different kind of interaction with CTAB micelles as compared to methoxy naphthalenes. The surfactant, viz., CTAB, forms spherical micelles in the presence of methoxynaphthalene (2−10 mM; 1:1), whereas in the presence of naphthols CTAB forms long worm-like micelles and even vesicles (discussed in a later part).

Microscopic Polarity at the Location of OH Groups of Embedded Naphthols. It is believed that while the aromatic rings of naphthols are embedded in micelles, the core of which having a dielectric constant around 2−7 only, the OH groups stand out toward the water region. NMR study also confirms that the aromatic ring of the naphthol resides near the nonpolar core in between tetraalkylammonium head groups of the surfactants. Although almost all of the previous studies on the

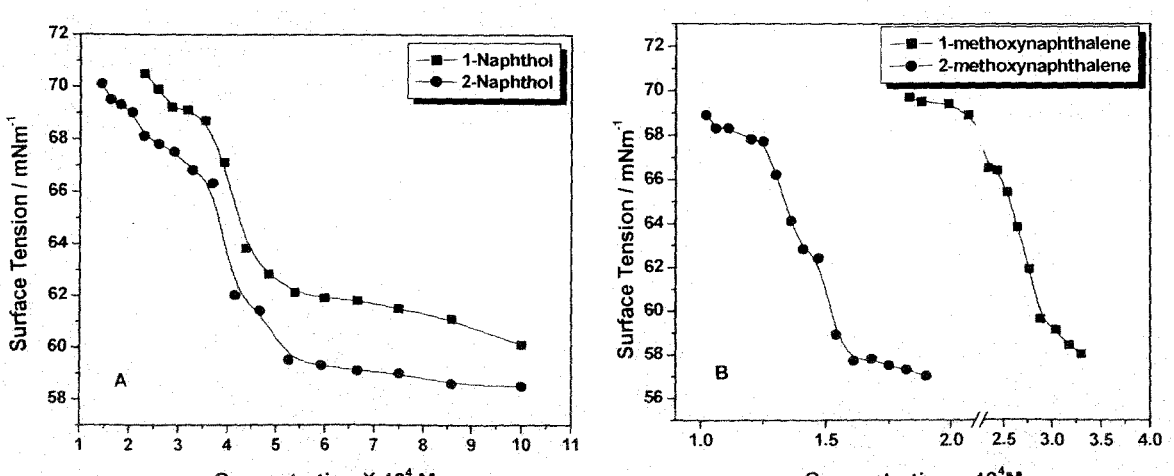

Figure 3. Surface tension of naphthols (A) and methoxynaphthalenes (B) as a function of concentration in water at 25 °C.

hydrotrope-induced microstructural transitions of micelles argue that the OH groups protrude out of the micellar surface and remain close to the aqueous layer, no experimental verification has so far been reported. To understand the exact nature of the location of the OH group, the micropolarity of the residence sites is determined. Spectral characteristics, especially fluorescence spectra, are often very sensitive to the environments around the probe molecule. Because of this, fluorescence spectroscopy has become one of the important methods for the study of the structure and dynamics of the microheterogeneous systems. Unfortunately, the excited state proton transfer process (ESPT) of hydroxyaromatic compounds, viz., 1- and 2-naphthols, complicates their spectral properties. The absorption spectra are also not sensitive to the environmental conditions in the present system. Moreover, information regarding the microenvironment of the aromatic π-electron system, which might have been obtained from the study of spectral characteristics, would not be helpful in determining the location of protruded OH groups of naphthol molecules. Therefore, pK_a shift of the acid–base equilibrium of the OH group of naphthols in a microheterogeneous medium relative to aqueous solution would be the ideal route for getting such information precisely. This shift in pK_a in a cationic micelle like CTAB relative to aqueous solution may be due to the surface potential of the micelle and the polarity variation at the micellar interface from that of the bulk (in the absence of any specific interaction). The theoretical background of the analysis of data pertaining to the interfacial acid–base equilibrium of naphthol molecules has been well documented for other similar probes.[26,27] While determining pK_a values of the present system, let us assume that the acid–base equilibrium of the OH group of naphthols is described by

$$\Phi OH + H_2O = \Phi O^- + H_3O^+ \qquad (1)$$

where ΦO^-, ΦOH, and H_3O^+ are deprotonated and protonated (neutral) forms of the naphthols and the proton, respectively. For the naphthol indicators in aqueous micellar solution, the apparent pK_a values were obtained from the change in the ultraviolet absorption spectra as a function of bulk aqueous pH by means of the following Henderson–Hasselbach equation (which considers only concentration terms at low concentration conditions) as follows (eq 1):

$$pK_a^{obs} = pH - \log[\Phi O^-]/[\Phi OH] \qquad (1a)$$

provided that the quantity $[\Phi O^-]/[\Phi OH]$ is determined by $(A - A_{\Phi OH})/(A_{\Phi O^-} - A)$, where A, $A_{\Phi OH}$, and $A_{\Phi O^-}$ are the absorbances of naphthols at experimental pH and low and high pH's, respectively. The near UV spectra of 1-naphthol as a function of the bulk aqueous pH in CTAB micelle solution are shown in Figure 4 (unfortunately, the spectral profile of 2-naphthol is insensitive toward bulk aqueous pH and, therefore, cannot be studied). For the acid–base equilibrium of the interfacially located organic molecule, the pK_a^{obs} is now separated into two components, viz., an electrostatic component and a nonelectrostatic environmental component. This is formalized in relation 2

$$pK_a^{obs} = pK_a^0 - e\Psi_0/2.303kT \qquad (2)$$

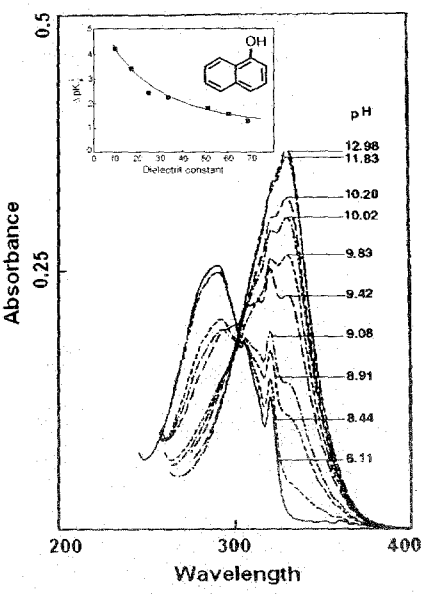

Figure 4. UV absorption spectra of 1-naphthol (0.5 mM) in 5.0 mM CTAB at varying pH.

where pK_a^0 is the apparent pK_a value if the surface potential of the micelle, Ψ_0, is null. Information can be obtained about the acid–base equilibrium at the surfactant–water interfaces by comparing pK_a^0 values of naphthols in the aqueous micellar systems with the pK_a values for naphthols in the aqueous–organic mixtures, e.g., dioxane–water mixtures. The apparent pK_a in organic–aqueous mixture, pK_a^m, is defined in the following relation (eq 3).

$$pK_a^m = B + \log U_H^0 - \log[\Phi O^-]/[\Phi OH] - \log \gamma^m_{\Phi O^-}/\gamma^m_{\Phi OH} \qquad (3)$$

where γ^m's are activity coefficient terms in the medium, B is the pH meter reading, and $\log U_H^0$ is the correction factor to be applied to pH meter reading to measure the actual hydrogen ion concentration in organic–aqueous mixtures. The pK_a^0 values relate to a system where the conjugate acid–base species reside in an interfacial microenvironment but the bulk aqueous solution pH is measured. Hence, the comparison between pK_a values in dioxane–water mixtures and pK_a^0 values in micelle systems should take into account the primary medium effect on the proton. In other words, pK_a^0 values need to compare to pK_a^i values rather than pK_a^m's where

$$pK_a^i = pK_a^m + {}_m\gamma_H^+ \qquad (4)$$

and ${}_m\gamma_H^+$ denotes the primary medium effect on the proton. It is usual to assume that the mean primary medium effect on HCl, ${}_m\gamma_\pm$, approximates to ${}_m\gamma_H^+$. The $\log U_H^0$ and ${}_m\gamma_\pm$ values given in refs 26 and 27 were employed to derive pK_a^i values in dioxane–water mixtures. These pK_a^i ($\Delta pK_a^i = pK_a^i - pK_a^w$) values as a function of medium dielectric constant are shown in Figure 4 (inset). The pK_a^0 values of 1-naphthol in CTAB micelles are determined with the aid of eq 2 and the known value of the surface potential of CTAB micelles of +141 mV.[26] The effective dielectric constant (D_{eff}) values are obtained by comparing ΔpK_a^0's (Table 1) of 1-naphthol on a micellar surface with ΔpK_a^i values in 1,4-dioxane–water mixtures (Figure 4; inset). It may be noted that D_{eff} values

TABLE 1: Results of pH Titration of 1-Naphthol in Aqueous and Aqueous CTAB Micellar Solution at 25°C

conc. of CTAB/mM (conc. of 1-HN = 0.5 mM)	pK_a^w	pK_a^{obs}	$-\Delta pK_a^{obs}$	pK_a^0	ΔpK_a^0
20		8.623	0.765	11.007	1.619
50	9.388	8.679	0.709	11.063	1.675
100		8.914	0.474	11.298	1.910

TABLE 2: D_{eff} Values of OH Group Location of Micellar Interface

conc. of CTAB/mM (conc. of 1-HN = 0.5 mM)	D_{eff}
20	51 ± 3
50	49 ± 3
100	45 ± 2

are measured on the basis of several assumptions: (i) both the protonated and deprotonated forms of the naphthol indicator are quantitatively partitioned into the micellar phase at least at high surfactant/naphthol ratio; (ii) the activity coefficient term ($\log \gamma^i_{\Phi O^-}/\gamma^i_{\Phi OH}$) is negligibly small so that ΔpK_a^0 values are directly comparable with the ΔpK_a^i behavior in different solvent dielectric constant bulk media; (iii) although the OH groups of naphthol protrude from the micellar surface, the acid−base equilibrium is still under the influence of micellar surface potential; (iv) it is evident that much like the 1,4-dioxane−naphthol system, the interfacial water of CTAB micelles forms H-bonds with micelle-embedded naphthols (discussed later), which act as a H-donor in both of the above cases. No serious error in the evaluation of D_{eff} due to the presence of this H-bond is thus anticipated because such an effect, if any, would be compensated by the similar interaction present in the reference system (naphthols in dioxane−water).

Table 2 shows that D_{eff} at the interface of CTAB micelles, as measured by the pK_a shift of interfacially located naphthols, varies from 51 ± 3 to 45 ± 2 as a function of CTAB concentration from 20 to 100 mM (concentration of naphthol being 0.5 mM throughout). This result indicates that naphthols are increasingly partitioned in micelles as the CTAB concentration is increased. Utilizing the solvatochromic visible absorption band maximum $E_T(30)$, D_{eff} estimates of 28−33 were obtained previously for CTAB micelles.[29] Therefore, in comparison to the previously determined micropolarity of the CTAB micellar surface (D_{eff} ~30), the present value of 45 (under conditions when most of the naphthol molecules are partitioned in micelles) is substantially high. This is an interesting observation. This clearly indicates that the OH groups are directed away from the surface of the micelles and are located around the more polar region. Assuming a polarity gradient to exist with the distance from the micellar surface, one can have a rough idea of the location of the OH groups in the Stern layer. A recent application of numerical Poisson−Boltzmann methods to the determination of the electrostatic potential and counterion distribution around polyelectrolyte such as DNA may be relevant in this respect.[30] In this case, the situation had prompted us to choose a dielectric constant "field", where low dielectric values exist near 30 at the polyelectrolyte surface and increase away to the values near 78.5 in bulk water. A rough estimation following the above work, which takes on a cylindrical polyelectrolyte (e.g., DNA) surface of radius 10 Å as the low dielectric region, shows that the present D_{eff} value of 45 (compared to ~30 at the micellar surface) could be rationalized assuming the OH group of naphthol to be protruded away from the CTAB micellar surface through a nearly 1 Å distance toward the Stern layer.[30]

Spectral Modification of Micelle-Embedded Dopants: Contribution of H-Bonding, $\pi-\pi$ or Cation$-\pi$ Interactions? In view of the differences in the viscoelastic responses and the morphological transitions of CTAB micelles (Figure 1) induced by neutral naphthols and the methoxy naphthalenes, UV absorption spectra of these dopants may be interesting to study in micellar media. To understand the kind of interactions which are operative in the micelle−dopant systems, the key element of the present study is to compare the spectral characteristics of naphthols (HNs which contain OH) with those of methoxy naphthalenes (MNs, which do not contain OH) under various conditions in order to visualize a consistent molecular picture eliminating the untenable suggestions. Aromatic compounds, e.g., naphthalene, in general, have two strongly overlapped bands in the near UV region, viz., the longitudinally polarized $^1L_a \leftarrow {}^1A$ band and the transversely polarized $^1L_b \leftarrow {}^1A$ band. While the vibrational structure of these bands appears differently in different substituted compounds, effects of extending conjugation in 1 and 2 positions by OH or CH_3O groups in naphthol and methoxynaphthalene molecules, respectively, are interesting. Both in 1-naphthol and 1-methoxy, naphthalene conjugation is extended in the transverse direction and, therefore, it affects the transverse polarized ^1L_a band. In 2-naphthol and 2-methoxy naphthalene, on the other hand, conjugation is primarily extended in the longitudinal direction, affecting both the intensity and the frequency of the longitudinally polarized ^1L_b band compared to the unsubstituted naphthalene.

It is well-known that the near UV spectra of aromatic compounds are affected by specific interactions like hydrogen bonding. Noncovalent interactions like $\pi-\pi$ and cation$-\pi$ also cause shifts in the electron distributions of the molecule. The OH group of naphthols can act as both a proton donor as well as a proton acceptor in forming intermolecular hydrogen bonding. A hydrogen bond in which the hydroxyl groups of naphthols is a proton donor releases electron density from the O−H bond toward the oxygen and hence, by an inductive effect, toward the aromatic ring. This causes a red-shift of the $\pi-\pi^*$ transition. Conversely, if a hydrogen bond is formed in which the hydroxyl oxygen is a proton acceptor, electrons are withdrawn from the naphthalene ring, and an opposite shift is anticipated. If both bonds could form at the same time and with equal ease, since their effects on the partial charges of the oxygen are opposite, the net change on the oxygen and hence on the aromatic ring may be small. Therefore, in such a situation, the spectral shift relative to the position of the band in a non-hydrogen-bonding situation ought to be small.[32] The near UV absorption of 1-naphthol which arises from two strongly overlapped $\pi-\pi^*$ transitions remains unaffected in the presence of submicellar aqueous CTAB solution, indicating the absence of any appreciable interaction (Figure 5) (the effect of CTAB micelles on the UV spectra of 2-naphthol is also similar). However, interestingly, significant red-shift starts to occur (6.4 nm at λ_{max} ~293 nm) in the presence of CTAB just above its cmc (0.96 mM) with a well-defined isobastic point at 296 nm. Such shifting of λ_{max} continues until most of the naphthol molecules are partitioned in the micellar phase at high surfactant/naphthol ratio (80:1; Figure 5A). The result suggests that the protruded OH groups of micelle-embedded naphthols form a H-bond with interfacially located (D_{eff} ~45) water molecules and act as a H-donor. It may also be argued that at a mole ratio of 1:1 of naphthol and the CTAB, at which maximum viscoelastic response is observed under shear due to the presence

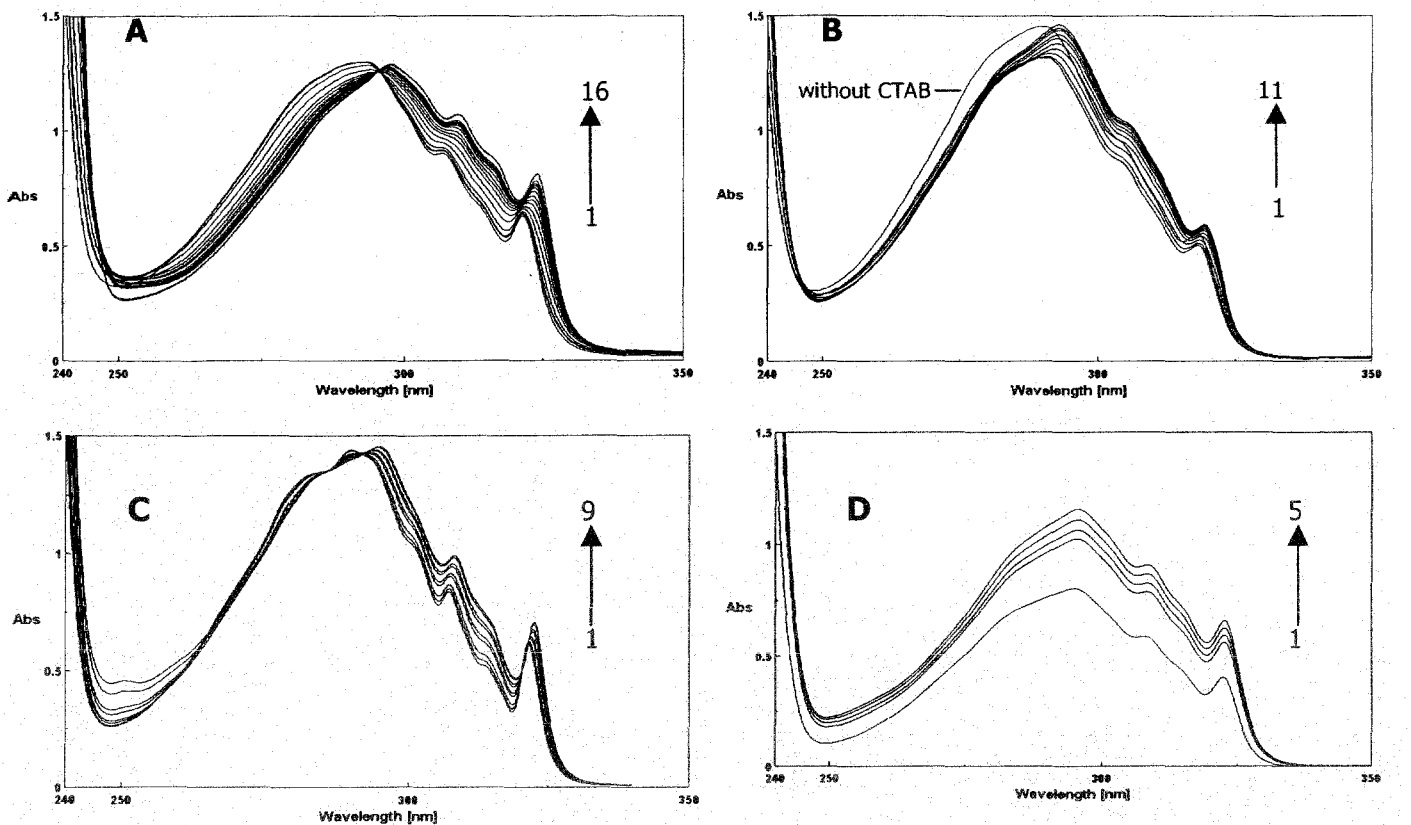

Figure 5. (A) Absorption spectra of 1-HN (0.25 mM) in water at varying concentrations of CTAB at 25 °C. [CTAB]: (1) 0.0, (2) 0.44, (3) 0.55, (4) 0.75, (5) 1.00, (6) 1.25, (7) 1.50, (8) 1.75, (9) 2.00, (10) 2.50, (11) 3.00, (12) 3.50, (13) 4.00, (14) 5.00, (15) 15.00, (16) 20.00 mM. (B) Absorption spectra of 1-MN (0.25 mM) in water at varying concentrations of CTAB at 25 °C. [CTAB]: (1) 0.33, (2) 0.50, (3) 0.75, (4) 1.00, (5) 1.50, (6) 2.00, (7) 2.50, (8) 3.00, (9) 3.50, (10) 4.00, (11) 5.00 mM. (C) Absorption spectra of 1-HN (0.25 mM) in isooctane at various concentrations of 1,4-dioxane at 25 °C. [Dioxane]: (1) 0.00, (2) 13, (3) 20, (4) 40, (5) 50, (6) 80, (7) 100, (8) 160, (9) 200 mM. (D) Absorption spectra of 1-HN (0.25 mM) in acetonitrile at different percentages of water at 25 °C. % of water: (1) 0.00%, (2) 4%, (3) 6%, (4) 8%, (5) 10%.

of entangled worm-like micelles, not all of the naphthol molecules are embedded in the micelles, but some are located in the palisade layer. These naphthols may, however, be involved in H-bond network formation with embedded molecules via interfacial water.

The spectral feature (Figure 5A) and the nature and degree of shift undoubtedly resemble the spectra of naphthol in isooctane at various dioxane concentrations (red-shift of 6.3 nm at λ_{max} ~293 nm, Figure 5C, as compared to a red-shift of 6.4 nm at λ_{max} ~293 nm, Figure 5A) where naphthol acts as the hydrogen bond donor and dioxane as the acceptor (Figure 5 C).[31]

Previously, it has been shown that, in the ground state, 1-naphthol interacts with water via oxygen, whereas with alcohols (ethanol and isopropanol) and acetonitrile it interacts via hydrogen from the hydroxyl group.[33] The nature of spectral modification encountered by micelle free naphthol molecules in the presence of water is shown in Figure 5D. This figure shows that on every addition of water (up to 10% v/v) substantial gain in intensity is displayed by 1-naphthol spectra (in acetonitrile) with little change of wavelength. The nature of spectral modification of 1-HN due to H-bond formation is quite different from that of micelle-embedded naphthol. It may be argued that, like alcohols and acetonitrile media, naphthols at the interface (D_{eff} ~45) act as H-donating agents and water as a H-acceptor at the oxygen atom. This is indeed interesting. The low D_{eff} value found for the interfacial microenvironment of CTAB micelles may be attributed to a low interfacial water activity. Nevertheless, it has also been argued that the low interfacial D_{eff} value may be a result of the H-bond donor properties of the water in the interfacial region being different from that of bulk water, and/or the presence of electrostatic image interactions caused by the proximity of the low dielectric hydrocarbon core. Present experiments indeed justify the former conjecture precisely.[34] It is known that the water molecules at the micellar interface have some strange properties.[35,36] The solvation dynamics are slowed down by several orders of magnitude relative to bulk water. The reorientational motion is also restricted. The dynamics of water molecules near an aqueous micellar interface has been a subject of intense current interest because such a system serves as a prototype of complex biological system. Furthermore, oxygen K absorption and emission spectra of water molecules in the micellar interface also show that the local electronic structure of water molecules is dramatically different from that of bulk water.[37] The relatively less polar and less mobile water molecules compared to bulk water form a strong H-bond with the OH group of embedded naphthols, which act as H-donors and result in an optimum orientation of aromatic π-electron systems in the micelles to shield the surfactant headgroup charges efficiently; maybe via cation$-\pi$ interaction; i.e., the cation charge of surfactant head groups interacts with the quadrupole moment of the aromatic π-system of naphthols. On the other hand, as the H atom of OH is replaced by a CH_3 group (viz., the methoxy naphthalene molecule), the ability of intermolecular H-bond formation disappears. Instead, the H-accepting tendency from a potential donor is enhanced. The nature of changes encountered in the UV spectra of methoxy naphthalenes on the addition of CTAB above its cmc indicates the permeation of the dopant molecules in the micelles (Figure 5B). The small red-shift compared to

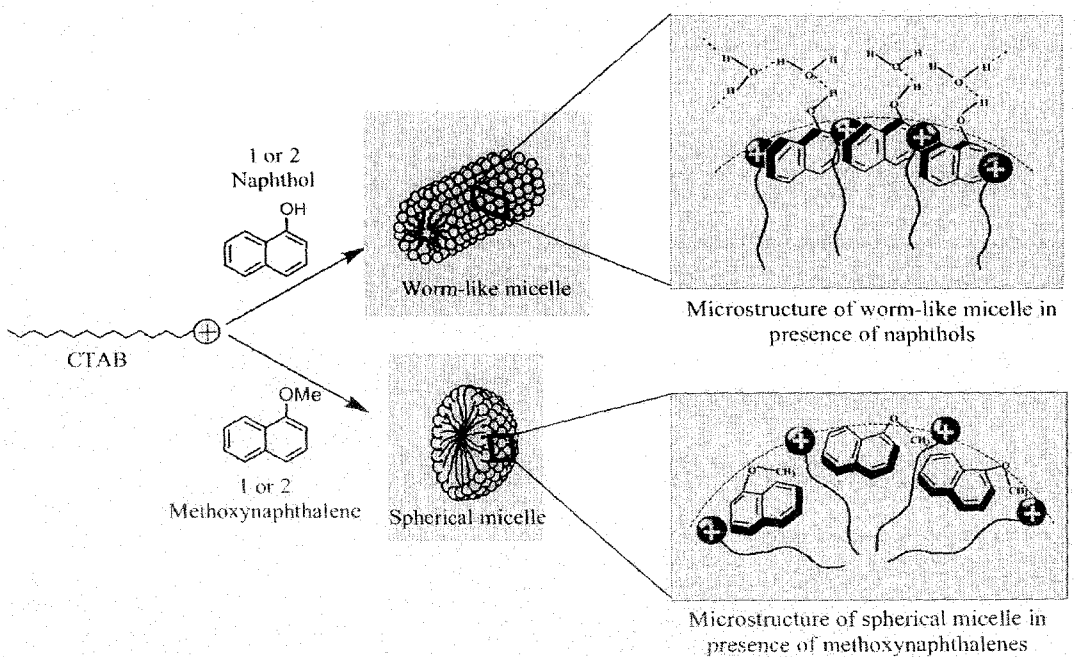

Figure 6. Schematic representation of the microstructures found in worm-like micelles formed by naphthols and spherical micelles formed by methoxynaphthalenes with CTAB.

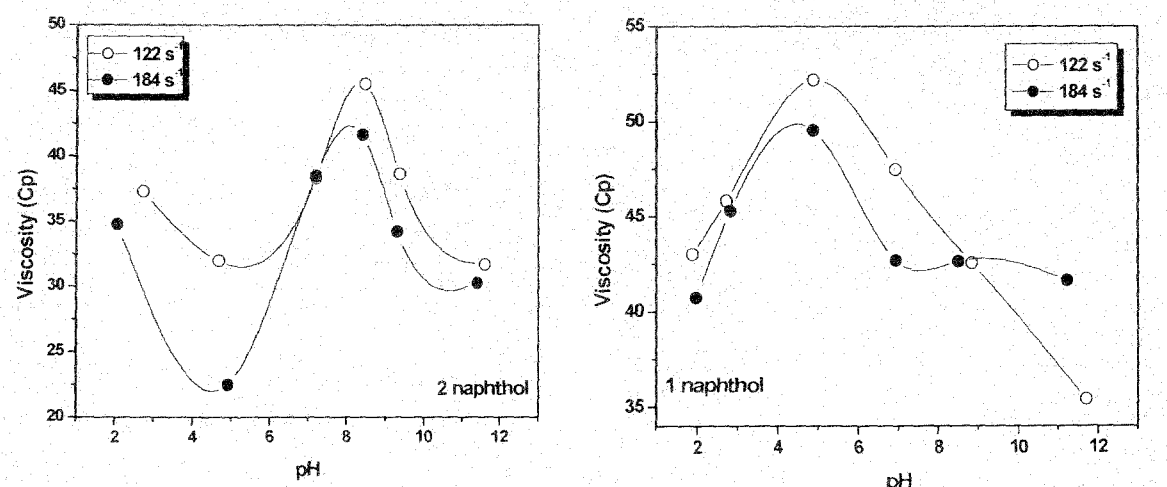

Figure 7. Viscosity vs pH profile for naphthol/CTAB systems at fixed shear rates of 122 and 184 s^{-1}.

that in naphthols indicates a weaker noncovalent interaction takes place. The large drop in intensity on first addition of 0.33 mM CTAB is the signature of breaking of a H-bond with bulk water molecules. Due to their directionality and spatial arrangement, complementary multiple H-bonding interactions at the micellar interface lead to engineering well-defined supramolecular structure via micellar headgroup charge shielding by π-electron systems of naphthols (Figure 6). This result of unusual H-bonding may be relevant, not only when considering the H-bonding of the interfacial water molecules in the specific micelle and dopant studied here but also for the H-bonding interaction of other micelle−dopant systems as well.

Shear-Induced Viscosity and pH. The role of neutral hydroxyaromatic dopants, viz., 1- and 2-HN, which are found to be efficient in bringing about microstructural transition in CTAB and CPB micelles, stimulates the idea of designing a route for pH-responsive vesicle formation.[5] This idea stems from the fact that the dopants, which under neutral conditions activate the formation of worm-like micelles at pH ~5.0, may on partial ionization of the OH group increase the packing parameter further via charge screening. This idea tempted us to study the pH dependent viscosity changes of the present viscoelastic gel system.[38] Figure 7 shows the viscosity−pH profiles of the 1-HN−CTAB and 2-HN−CTAB systems at constant shear of 122 and 184 s^{-1}, respectively. The general nature of the variation of viscosity as a function of pH for both 1- and 2-naphthol−CTAB systems is similar in high shear regime (viz., 122 and 184 s^{-1}, respectively). However, morphological responses are not identical for both of the systems. While the viscosity of both, 2- as well as 1-HN−CTAB systems, is quite high (35−45 Cp) due to formation of long worm-like micelles at low pH, the viscosity of the former system falls initially, indicating formation of shorter micelles with pH until pH ~5.0 is reached. On the other hand, for 1-HN−CTAB, the onset of viscosity rise as a function of pH is found to occur from very low pH (pH ~2.0). For 2-naphthol−CTAB, the onset of viscosity rise is observed at higher pH (>5.0) and the viscosity−pH profile passes through a maximum at pH ~8.5. The onset of viscosity rise is observed due to the partial titration of OH group, leading to charge screening of surfactant head groups by the naphtholate anion and at pH ~8.5 the worm-like micelles grow maximum. Further increase in pH results in the ionization of OH group further,

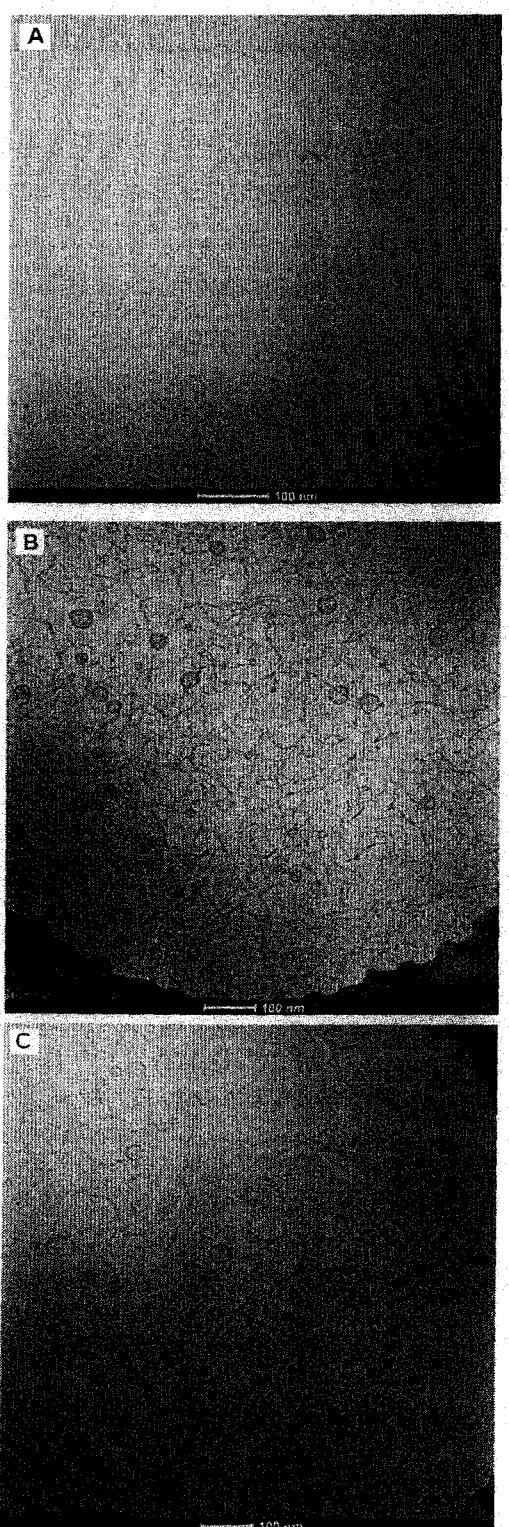

Figure 8. cryo-TEM micrographs of the CTAB−2-naphthol system (10 mM, 1:1) at normal pH (~5.5) (A) and at high pH (~9.4) (B). Part C shows linearly elongated worm-like micelles under shear flow.

and the packing parameter probably exceeds the critical value of 1/2 via enhanced charge screening, leading to vesicle formation (for naphthols, $pK_a > 9$, which means 50% ionization of the OH group at pH ~9.0). This results in the fall of viscosity of the system. Since 1-naphthol could modulate the micellar surface curvature more efficiently, a little dissociation of the OH group (at low pH range) leads to an appreciable decrease of surface curvature via charge screening and promotes long worm-like micelle formation. In fact, for the 1-HN−CTAB system, vesicles start to form even at slightly higher than pH ~5.0 (Figure 7). A simple and effective route to design pH-responsive viscoelastic worm-like micelles and less viscous globular vesicles based on naphthol dopants may be tuned by controlling the degree of charge screening of CTAB micelles via controlled ionization of naphtholic OH groups. The result of pH-responsive morphology modification is further investigated by means of cryo-TEM.

Cryogenic Transmission Electron Microscopic Study. Cryo-TEM images of the CTAB−2-naphthol system at low and high pH's are shown in Figure 8. At low pH (pH ~5.5), the micrograph looks like a condense, isotropic, and continuous network (Figure 8A) of worm-like micelles along with monodisperesed vesicles of very short diameters.

The micelles are slightly entangled. At high pH (pH~9.4), the system contains very long (endless in micrograph) worm-like micelles, which coexist with large unilamellar vesicles. This is undoubtedly due to enhanced charge screening of micelles by naphtholate anions. The field is seen to populate mainly by large vesicles of diameter ~30 nm along with thinly populated smaller vesicles. It is also seen that the long worm-like micelles are highly entangled. Sometimes they are found to elongate linearly under shear flow (Figure 8c). The solutions are completely transparent. The direct imaging by cryo-TEM supports the rheological observation as a function of pH (Figure 7). At low pH, the worm-like micelles are formed via headgroup charge shielding by aromatic π electrons, whereas, at high pH, ionization of OH groups takes place and the packing parameter exceeds the critical value of 1/2 via enhanced charge screening by naphtholate ion. This leads to unilamellar vesicle formation along with long worm-like micelles.

Conclusion

Neutral naphthols and methoxynaphthalenes, both with an aromatic π-system in their structures, are fairly surface active and embedded in aqueous CTAB micelles strongly. However, unlike methoxynaphthalenes, only naphthols can promote spherical to long worm-like micellar transition at room temperature and impart strong viscoelasticity and unusual rheology to the system. The success of naphthols in effecting microstructural transition of micelles lies in their unique ability to form H-bonds with interfacial water molecules, which have shown unusual H-bond donating properties compared to bulk water. The OH groups of micelle-embedded naphthols are protruded toward the Stern layer through ~1 Å and the dielectric constant of OH sites has been measured as 45 ± 2 by observing the pK_a shift of acid−base equilibrium of naphthols at the interface relative to that in bulk water. The result of unusual H-bonding may be relevant, not only when considering the H-bonding of the interfacial water molecules in the specific micelle and dopant studied here but also for the H-bonding interaction of other micelle−dopant systems as well. On the basis of hydroxyaromatic dopants like naphthols, a simple and effective route to design pH-responsive viscoelastic worm-like micelles and the vesicles of single tail cationic surfactant (CTAB) is reported. Results are confirmed by observing cryogenic transmission electron microscopy (cryo-TEM) images.

Acknowledgment. The authors are thankful to Council of Scientific and Industrial Research, New Delhi, for financial support. Dr. Wins Busing of FEI Company, The Netherlands, is gratefully acknowledged for help in acquiring the cryo-TEM data.

References and Notes

(1) Hoeben, F. J. N.; Jonkheijin, P.; Meijer, E. W.; Schenning, A. P. J. H. *Chem. Rev.* **2005**, *105*, 1491–1498.
(2) Guldi, D. M.; Zerbetto, F.; Georgakilas, V.; Prato, M. *Acc. Chem. Res.* **2005**, *38*, 38–42.
(3) Yoosaf, K.; Belbakra, A.; Nichola, A.; Llanes-Pallas, A. *Chem. Commun.* **2009**, 2830–2832.
(4) Cui, S.; Liu, H.; Gan, L.; Li, Y.; Zhu, D. *Adv. Mater.* **2008**, *20*, 2918–2923.
(5) Saha, S. K.; Jha, M.; Ali, M.; Chakraborty, A.; Bit, G.; Das, S. K. *J. Phys. Chem. B* **2008**, *112*, 4642–4647.
(6) Tan, G.; Ford, C.; John, V. T.; He, J.; McPherson, G. L.; Bose, A. *angmuir* **2008**, *24*, 1031–1036.
(7) Isayama, M.; Nomiyama, K.; Yamaguchi, T.; Kimizuka, N. *Chem. tt.* **2005**, *34*, 462–463.
(8) Singh, M.; Ford, C.; Agarwal, V.; Fritz, G.; Bose, A.; John, V. T.; Pherson, G. L. *Langmuir* **2004**, *20*, 9931–9937.
(9) Clint, J. H. *Surfactant Aggregation*; Blakie & Son Ltd.: London, 1992; p 147.
(10) Manohar, C. In *Micelles, Microemulsions and Monolayers, Science and Technology*; Shah, O. D., Ed.; Marcel Dekker, Inc.: New York, 1998; p 145.
(11) Davis, T. S.; Ketner, A. M.; Raghavan, S. R. *J. Am. Chem. Soc.* **2006**, *128*, 6669–6675.
(12) Tung, S.-H.; Lee, H.-Y.; Raghavan, S. R. *J. Am. Chem. Soc.* **2008**, *130*, 8813–8817.
(13) Israelachivili, J. N.; Mitchell, D. J.; Ninham, B. N. *J. Chem. Soc., Faraday Trans. 2* **1976**, *72*, 1525–1568.
(14) Rehage, H.; Hoffman, H. *J. Phys.Chem.* **1988**, *92*, 4712–4719.
(15) Rehage, H.; Hoffman, H. *Mol. Phys.* **1991**, *74*, 933–943.
(16) Cates, M.; Candau, S. J. *J. Phys.: Condens. Matter* **1990**, *2*, 6869–6877.
(17) Hu, Y.; Rajaram, C. V.; Wang, S. Q.; Jamieson, A. M. *Langmuir* **1994**, *10*, 80–85.
(18) Ketner, A. M.; Kumar, R.; Davies, T. S.; Elder, P. W.; Raghavan, S. R. *J. Am. Chem. Soc.* **2007**, *129*, 1553–1557.
(19) Keller, S. L.; Boltenhagen, P.; Pine, D. J.; Zasadzinski, J. A. *Phys. Rev. Lett.* **1998**, *80*, 2725–2728.
(20) Boltenhagen, B.; Hu, Y.; Matthys, E. F.; Pine, D. J. *Phys. Rev. Lett.* **1997**, *79*, 2359–2362.
(21) Liu, C.; Pine, D. J. *Phys. Rev. Lett.* **1996**, *77*, 2121–2124.
(22) Zheng, Y.; Lin, Z.; Zakin, J. L.; Talmon, Y.; Davis, H. T.; Scriven, L. E. *J. Phys. Chem. B* **2000**, *104*, 5263–5271.
(23) Mendes, E.; Narayanan, J.; Oda, R.; Kern, F.; Candau, S. J. *J. Phys. Chem. B* **1997**, *101*, 2256–2258.
(24) Agarwal, V.; Singh, M.; McPherson, G.; John, V.; Bose, A. *Colloids Surf., A* **2006**, *281*, 246–253.
(25) Dougherty, D. A. *Science* **1996**, *271*, 163–168.
(26) Drummond, C. J.; Grieser, F.; Healy, T. W. *J. Chem. Soc., Faraday Trans. 1* **1989**, *85*, 521–535.
(27) Drummond, C. J.; Grieser, F.; Healy, T. W. *J. Chem. Soc., Faraday Trans. 1* **1989**, *85*, 537–550.
(28) Mishra, B. K.; Samant, S. D.; Pradhan, P.; Mishra, S. B.; Manohar, C. *Langmuir* **1993**, *9*, 894–898.
(29) Drummond, C. J.; Grieser, F.; Healy, T. W. *Faraday Discuss. Chem. Soc.* **1986**, *81*, 95–102.
(30) Lamm, G.; Pack, G. R. *J. Phys. Chem. B* **1997**, *101*, 959–965.
(31) Baba, H.; Suzuki, S. *J. Chem. Phys.* **1961**, *35*, 1118–1127.
(32) Nemethy, G.; Ray, A. *J. Phys. Chem.* **1973**, *77*, 64–68.
(33) Zharkova, O. M.; Korolev, B. V.; Morozova, Y. P. *Russ. Phys. J.* **2003**, *46*, 68–74.
(34) Ramachandran, C.; Pyter, R. A.; Mukherjee, P. *J. Phys. Chem.* **1982**, *86*, 3198–3205.
(35) Bhattacharya, K. *J. Fluoresc.* **2001**, *11*, 167–179.
(36) Balasubramanian, S.; Pal, S.; Bagchi, B. *Curr. Sci.* **2002**, *82*, 845–848.
(37) Gasjo, J.; Anderson, E.; Forsbeing, J.; Aziz, E. F.; Brena, B.; Johansson, C.; Nordgren, J.; Duda, L.; Adersson, J.; Hennies, F.; Rubensson, J.; Hansson, P. *J. Phys. Chem. B* **2009**, *113*, 8201–8205.
(38) Lin, Y.; Han, X.; Huang, J.; Fu, H.; Yu, C. J. *Colloid Interface Sci.* **2009**, *330*, 449–455.

JP907677X